Volume 9, Issue 2, 2020, 988 - 994 ISSN 2284-6808

Letters in Applied NanoBioScience

https://nanobioletters.com/

https://doi.org/10.33263/LIANBS92.988994

Original Research Article Open Access Journal

Received: 08.05.2020 / Revised: 04.05.2020 / Accepted: 05.05.2020 / Published on-line: 10.05.2020

Antibacterial and antibiofilm activity of probiotic based silver nanoparticles is a green approach in biomedical applications

Tania Thabeeda Subhanandaraj [1], Keerthi Thalakattil Raghavan [2,*], Rakhie Narayanan [1]

[1] School of Biosciences, Mahatma Gandhi University, Kottayam, Kerala- 686560, India

[2] School of Biosciences, Mahatma Gandhi University, Kottayam, Kerala- 686560, India

*corresponding author e-mail address: ***keerthithalakattilraghavan@gmail.com***

ABSTRACT

Biosynthesis of nanoparticles is not a new approach in nanotechnology. Stability, size, catalysis ability, non-toxicity, biocompatibility and speed of synthesis are the facts considering while selecting the method of synthesis for medical applications. Probiotics are beneficial microorganisms that comes under generally regarded as safe status. The ability of two probiotic bacteria *Bacillus clausii* and Bacillus *subtilis* from Enterogermina® is tested for its ability to synthesize silver nanoparticles and its biological applications. Synthesis was confirmed by UV- Vis spectroscopy, FTIR, XRD, SEM- EDX and TEM. The biosynthesized silver nanoparticles showed good antibacterial activity against all the gram negative pathogens tested but not to *Staphylococcus aureus.* Even though *S. aureus* was not inhibited, its biofilm formation was inhibited by the AgNPs. AgNPs also exhibited a dose dependent antioxidant activity. The antibacterial, antibiofiilm and antioxidant properties of biosilver nanoparticles extended their applications in medical field especially in catheters and dental cares.

Keywords: *Probiotics; silver nanoparticles; antibacterial activity; antibiofilm activity.*

1. INTRODUCTION

Nanotechnology is an emerging field of research which attains maximum growth in the previous few decades. The most important factor which contributes to the activity of nanoparticles is its size usually below 100nm. There are different methods for the synthesis of nanoparticles: physical, chemical and biological. As physical and chemical methods are expensive, time consuming and involves the use of hazardous chemicals, nanobiotechnology evolved as a solution to this. Plant extracts, bacteria, fungi and algae can mediate the reduction of metal salts to ions and can scale up them to nanosized particles [1]. Antibacterial property of silver is known to man from the early days. Silver salts mostly $AgNO_3$ is using in treating burns, for water sterilization, in cosmetics etc. It was advised in the USA that 1% $AgNO_3$ must be instilled in newborns eye immediately post delivery [2]. Recently silver found tremendous applications in medicine and health care products and there are several patented products which includes silver coated medical devices, silver based wound dressings, personal care products such as sanitary towels, cosmetics, tooth brushes, hair dyes, antimicrobial food packaging etc.[3].

The attempt to fabricate silver salts to metal nanoparticles developed recently. The high surface area volume ratio added the demand for nanoparticle formulations as it provides more surface to react with other molecules. The scientific community is in continuous search for biocatalysts for the synthesis of nanoparticles. Bacteria mediated synthesis is gaining importance as it is suitable for mass production, biocompatibility and no toxicity [4]. Since most of the bacteria reported to have the property of nanoparticle synthesis belongs to the pathogen group, selection of a bacteria with GRAS (generally regarded as safe) status will reduce the risk.

In our study two probiotic bacteria *Bacillus clausii* and *Bacillus subtilis* isolated from a probiotic formulation Enterogermina® was used. Probiotics are "live microorganisms which when consumed in adequate amounts confer health benefit to the host" [5]. The study aims to evaluate the ability of two strains to synthesize silver nanoparticles (AgNPs) and their antibacterial effects.

2. MATERIALS AND METHODS

2.1. Synthesis of probiotic mediated silver nanoparticles.

B. clausii and *B. subtilis* isolated from a probiotic formulation Enterogermina® was used for the synthesis of AgNPs. Bacterial cells as well as cell free supernatants were used as catalysts for the reduction of $AgNO_3$ to metallic silver [6, 7]. Bacterial cells and cell free supernatants were obtained by inoculating the strains into nutrient broth at 1% inoculums and incubated at 37ºC for 24hr. Cells were harvested by centrifuging at 10000rpm for 10min at 4ºC. Supernatants were collected and pellets were washed in PBS 2 times. Approximately 2gm wet mass of cells was added into 500ml of 1mM $AgNO_3$ solution.30ml of culture supernatant and 70ml $AgNO_3$ was mixed and both the suspensions were incubated at room temperature in dark and light under static and shaking condition and visually observed for 72hrs for color change. 1mM $AgNO_3$ without cells or supernatant was maintained as control. The flasks showed reddish brown color were sonicated for 3min with 30s cycle and 10s interval. Samples were centrifuged at 10000rpm for the removal of cell debris and the supernatant was again centrifuged at 15000rpm for 15 minutes. The pellets were collected and dispensed in deionized water for further analysis.

2.2. Characterization of AgNPs.

2.2.1. UV- Vis Spectroscopy.

Reduction of $AgNO_3$ was confirmed by UV-Vis Spectra of diluted samples ranging from 300- 600nm using Shimadzu UV 2600 spectrophotometer. Baseline was set with deionized water. AgNPs exhibit a characteristic Surface Plasmon Resonance peak (SPR) depending on its size.

2.2.2. Fourier Transform Infrared (FTIR) Spectroscopy.

The stretching and vibrations of capping biomolecules of AgNPs were detected by FTIR. FTIR spectrums of the diluted samples were taken in Shimadzu IS prestige ranging from 750-4500 $cm^{-1}$with a resolution of $1cm^{-1}$.

2.2.3. X-Ray diffraction (XRD).

The diluted sample was coated over a clean sterile glass slide and dried. XRD analysis was performed in RigakuMiniflex 600 X Ray diffractometer with Bragg's angle 2θ between 5° and 90° operating at a voltage of 40kV and a current of 15mA with Cu-kα radiation (λ= 1.5406nm).

2.2.4. Electron Microscopy.

Morphology and size of the AgNPs were determined by Scanning Electron Microscopy (SEM) coupled with Electron Dispersive X Ray (EDX) detection and High Resolution Transmission Electron Microscopy (HR-TEM). For SEM EDX samples were coated with gold and viewed under JEOL- JSM- 6390 microscope with an accelerating voltage of 20kV. High resolution TEM analysis was performed in JEOL- JEM-2100 with an accelerating voltage of 200kV. A drop of the sample was placed on carbon coated copper grid and kept for drying and later visualized.

2.3. Antibacterial activity of Probiotic AgNPs.

Antibacterial activity of probiotic AgNPs against selected human pathogens procured from Microbial Type Culture Collection (MTCC), Chandigarh, India was done by agar well diffusion. Overnight culture of *Escherichia coli* (MTCC 1610), *Salmonella typhi* (MTCC 733), *Pseudomonas aeruginosa* (MTCC 2453), *Staphylococcus aureus* (MTCC 1430) and *Klebsiellapneumoniae* (MTCC 432) in peptone water was plated on Muller Hinton Agar using sterile cotton swabs and wells of 7mm diameter were cut on it. Different volumes of nanoparticles (10µl, 20µl, 40µl and 80µl) were added into the wells and incubated at 37ºC for 24 hrs. Culture supernatants of *B. clausii* and *B. subtilis* were maintained as controls. The zone of inhibition around the wells was measured.

2.4. Determination of minimum inhibitory concentration (MIC).

MIC of probiotic AgNPs was determined by resazurin dye. Growth of pathogens in the presence of nanoparticles was evaluated by taking absorbance at 560nm. Detection of MIC by resazurin was done according to Loo *et al* with modifications [8]. The same volumes of nanoparticles used in agar well diffusion were added to 100 µl of overnight grown pathogens having OD of 1 in 96 well microtitre plate and incubated at 37ºC for 24 hrs. After incubation 30 µl of resazurin (1.5mg/10ml) was added to each well and incubated for 1 hr. development of pink color after incubation indicated live bacterial cells while blue or purple color indicated dead cells.

2.5. Antibiofilm activity.

Inhibition of pathogen biofilm production by AgNPs was done by microtitre plate assay [9, 10]. Briefly, 100µl of fresh nutrient broth (NB) was added to 10µl of overnight grown pathogen in 96 well polystyrene plate. Different volumes of AgNPs used in the previous experiments were make up to 100µl in order to maintain the volume constant and added to it and incubated at 37ºC for 24hrs. After incubation the planktonic pathogenic cells were removed by gentle pipetting without disturbing the biofilm and washed three times with sterile distilled water. 200µl of methanol was added to each well to fix the adherent cells and kept for 15 minutes, air dried and stained with 2% crystal violet for 15 minutes. Excess stain was removed by washing with distilled water. The adherent stain was extracted with 160µl of 33% glacial acetic acid and OD was measured at 595nm. Pathogens without AgNPs were maintained as control. Percentage inhibition of biofilm formation was calculated using the formula

$$\%\ inhibition = 100 - \{(ODoftest/ODofcontrol) \times 100\}$$

2.6. Free radical scavenging activity by 2, 2-diphenyl-1-picrylhydrazyl (DPPH) scavenging.

Antioxidant activity of probiotic AgNPs was determined by DPPH scavenging [11]. 1 ml of nanoparticle samples (concentration the same as mentioned above) were added to 1 ml of 1mM freshly prepared methanolic DPPH solution, vortexed and incubated in dark at room temperature. Optical density was measured at 517 nm. DPPH solution without test sample was maintained as control. The percentage DPPH scavenging activity was calculated by

$$\%\ DPPH\ scavenging = \left\{\frac{(ODofcontrol - ODoftest)}{ODofcontol}\right\} \times 100$$

2.7. Statistical evaluation.

All tests were done in triplicates and values are expressed as average ± standard deviation

3. RESULTS

3.1. Synthesis of probiotic mediated silver nanoparticles.

Primary confirmation of AgNPs formation was done by visual observation. Flasks inoculated with culture supernatant and $AgNO_3$ did not show any colour change. Brown to brick red colour was formed in flasks inoculated with bacterial cells and $AgNO_3$after 24 hrs of incubation in light (Fig 1 and 2) in static as well as shaking conditions. Both probiotics *B. clausii* and *B. subtilis* were able to reduce $AgNO_3$ into metallic silver. Colour of $AgNO_3$ solution which was maintained as control did not change after 24 hrs of incubation in light and dark condition. Sonication of the samples disrupts the bacterial cells and releases the nanoparticles synthesized inside the cell. Centrifugation at 10000rpm removed larger cell debris and centrifugation at higher rpm pelletized the nanoparticles.

3.2. Characterization of AgNPs.

The UV Visible spectroscopy analysis of *B. clausii* and *B. subtilis* silver nanoparticles showed absorption maximum or Surface Plasmon Resonance (SPR) peak at 415 nm and 419 nm respectively (Fig 3).

Figure 1. Before incubation.

Figure 2. After incubation brown to red colour was formed.

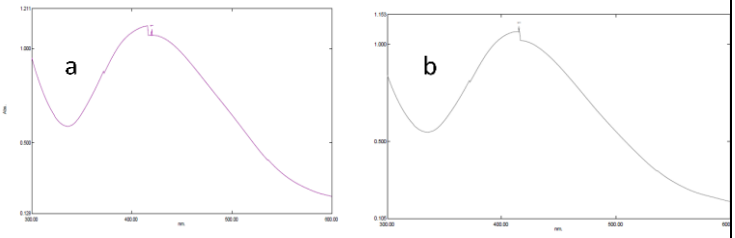

Figure 3. a) SPR peak of *B. clausii* at 415 nm and b) SPR peak of *B. subtilis* at 419 nm.

3.2.1. FTIR.

FTIR was done to know the nature of organic molecules associated with silver nanoparticles. FTIR spectrum of *B. clausii* (Fig 4) and *B. subtilis*(Fig 5) AgNPs showed strong absorption peaks in between 3000 and 4000 cm^{-1} due to the stretching vibrations of amines and their corresponding bending vibration is assigned to 1633 cm^{-1} [12]. The other major peaks between 3000-2850 cm^{-1} correspond to the C-H stretching.

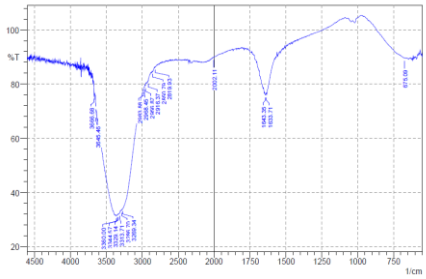

Figure 4. FTIR of *B. clausii* AgNPs.

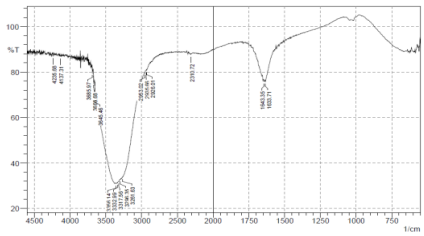

Figure 5. FTIR of *B. subtilis* AgNPs.

3.2.2. X- Ray Diffraction pattern.

Silver nanoparticles are usually Face Centered Cubic (FCC) crystalline structures. Fig 6 and fig 7 represents XRD pattern of *B. clausii* AgNPs and *B. subtilis* AgNPs respectively. *B. clausii* AgNPs exhibited Bragg's reflection at 27.77˚ and 32.18˚ which is a shift in miller indices from FCC due to the presence of organic molecules or strain generated during the sample preparation [13]. *B. subtilis* AgNPs exhibited 2θ angles at 35.63º which is also a shift due to the above mentioned reasons.

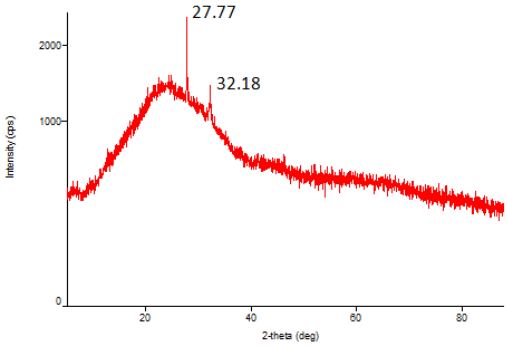

Figure 6. XRD pattern of *B. clausii* AgNPs.

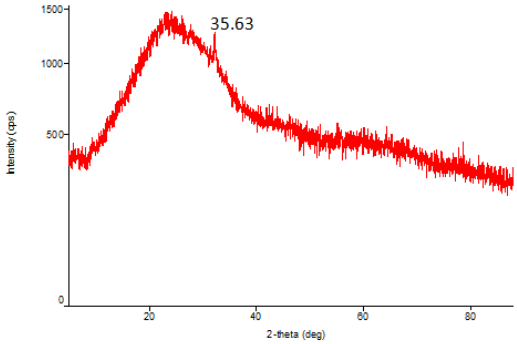

Figure 7. XRD pattern of *B. subtilis* AgNPs.

3.2.3. Electron Microscopy.

SEM EDX and HR-TEM studies revealed the morphology and size of biosynthesized AgNPs. SEM images showed the formation of nanoparticles in cell debris and the presence of elemental silver was confirmed by EDS. The peak at 3keV is the characteristics of metallic silver in EDX.

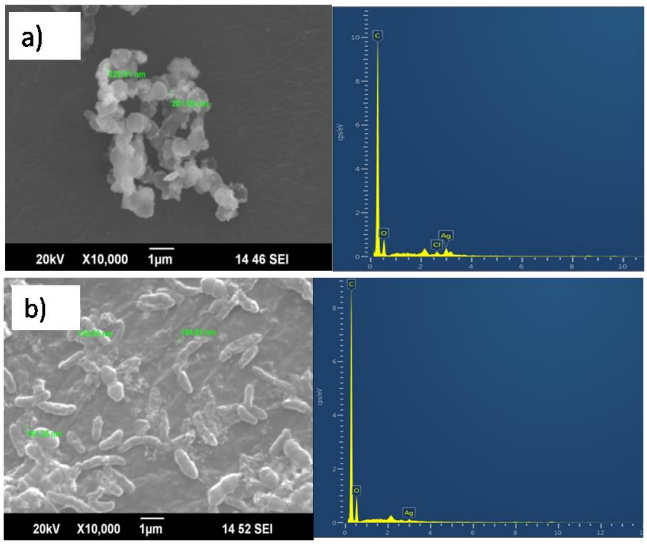

Figure 8. SEM-EDX of *B. clausii* (a) and *B. subtilis* (b) AgNPs. AgNPs can be seen among cell debris and the EDX spectrum confirms the presence of silver.

Fig 8 shows the characteristic peak of metallic silver synthesized by *B. clausii* and *B. subtilis* respectively. The other peaks in EDX are an indication of elements present in the sample. HR- TEM images of the both nanoparticles showed well dispersed and spherical nanoparticles with diameter between 20- 50 nm. TEM image of *B. subtilis* AgNP also showed that they are synthesized extracellularly or intracellularly and later secreted outside the cell but attached to the capsular material (Fig 9).

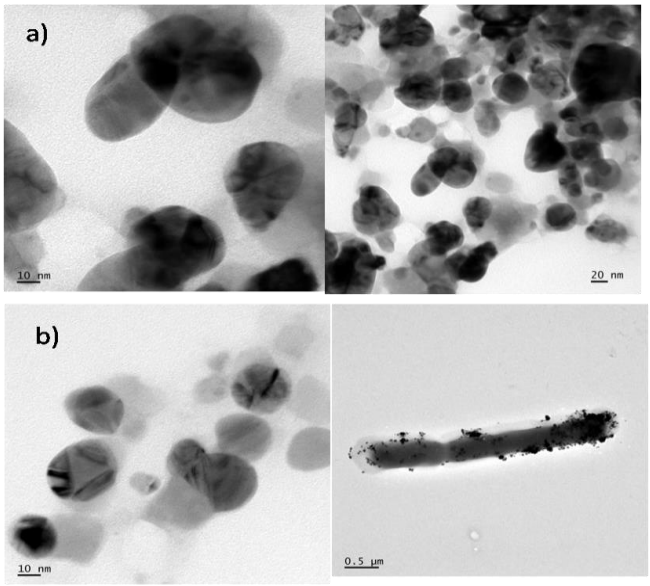

Figure 9. TEM images of *B. clausii* and *B. subtilis* AgNPs. The size of AgNPs ranges between 20-50nm

3.3. Antibacterial activity.

The probiotic silver nanoparticles were able to inhibit the pathogens except *S. aureus*. As the concentration/volume of nanoparticles increases the diameter of the zone of inhibition also increases (Table 1). Maximum zone of inhibition was shown by 80µl of the nanoparticle. But the control wells (in the middle of Petri dishes) didn't show any zone (Fig 10) which showed that the antibacterial activity is not due to the probiotic bacteria or its extracellular components but the silver nanoparticles synthesized by them.

3.4. Minimum inhibitory concentration.

MIC detection by resazurin dye confirmed the inhibition of growth of pathogens by probiotic AgNPs. Blue or purple colour represents the dead cells and pink colour represents live cells. Interaction of pathogens with different volumes of AgNPs resulted in cell death. As shown in fig 11,10 µl, 20 µl, 40 µl and 80 µl of both AgNPscan inhibit the pathogen growth but not *S.aureus* and the result is comparable with agar well diffusion test where no zone of inhibition was found for *S. aureus.*10 µl of crude AgNPs was sufficient for killing the pathogens in 24 hrs.

3.5. Antibiofilm activity.

Inhibition of pathogen biofilm formation by AgNPs was concentration dependent. As the concentration of nanoparticles increases the percentage of biofilm inhibition also increases. *B. clausii* and *B. subtilis* culture supernatants were not much effective in inhibiting the biofilm. *P. aeruginosa* biofilm was most susceptible to the nanosilver while *S. aureus* the least susceptible. Low concentrations of AgNPs (10µl) inhibited *E. coli* and *S. aureus* biofilms the most. *B. clausii* AgNPs inhibited *E. coli* and *S. aureus* by 69.29% and 60% respectively whereas *B. subtilis*AgNPs inhibited 39.54% ad 31.7% respectively. But at higher concentration (80µl) of both AgNPs above 80% of *S. aureus* biofilm was inhibited and more than 90% of *K. pneumoniae* and *P. aeruginosa* biofilms was inhibited at the same concentration.

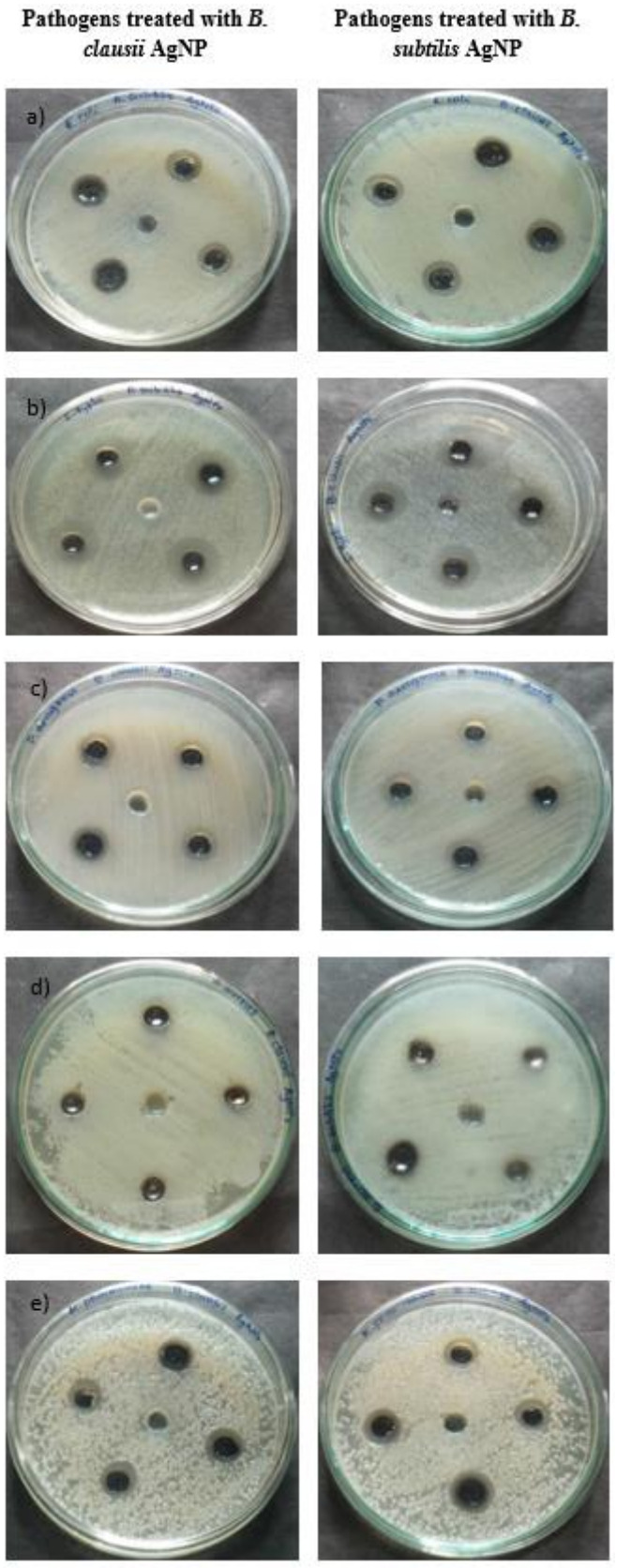

Figure 10. Zone of Inhibition of pathogens (a) *E. coli*, (b) *S. typhi*, (c) *P. aeroginosa*, (d) *S. aureus*, (e) *K. pneumonia.*

3.6. Antioxidant activity by DPPH method.

Antioxidant activity was performed to determine the free radical scavenging activity of nanoparticle samples. As the concentration of nanoparticles increases, antioxidant activity decreases. The highest antioxidant activity was shown by 10µl volume of nanoparticle synthesized by both *B. clausii* and *B. subtilis*. The percentage of scavenging was shown in table 4.

3.7. Discussion.

Green synthesis of silver nanoparticles is achieved through plant extracts, bacteria, fungi, yeast and cyanobacteria. The biomolecules from these sources not only reduces silver salts to silver but also provide additional benefits as it prevents agglomeration of nanoparticles by capping, reduces toxicity, and increases the antimicrobial activity [14]. Bacteria is an excellent and reliable catalyst for nanoparticle synthesis. Extracellular synthesis of AgNPs is mediated through the components or enzymes secreted outside the bacterial cells and it is achieved by cell free supernatants but some bacteria synthesize nanoparticles intracellularly also [15]. Fang et al., [16] explained that silver ions interact with bacterial cell wall components or extracellular proteins or with intracellular proteins or cofactors to reduce it to metallic silver nanoparticles. One of the most accepted mechanisms in bacterial synthesis is the reduction of silver nitrate by cytoplasmic nitrate reductase ezyme. An insilico study by Mukherjee et al., [17] revealed the interaction between nitrate reductase and $AgNO_3$. The strong binding of enzyme and silver nitrate produces AgNPs. *B. subtilis* and *B. clausii* produce AgNPs intracellularly but TEM analysis (fig: 9b) of *B. subtilis* gives a clue that they are secreted outside the cell surface.

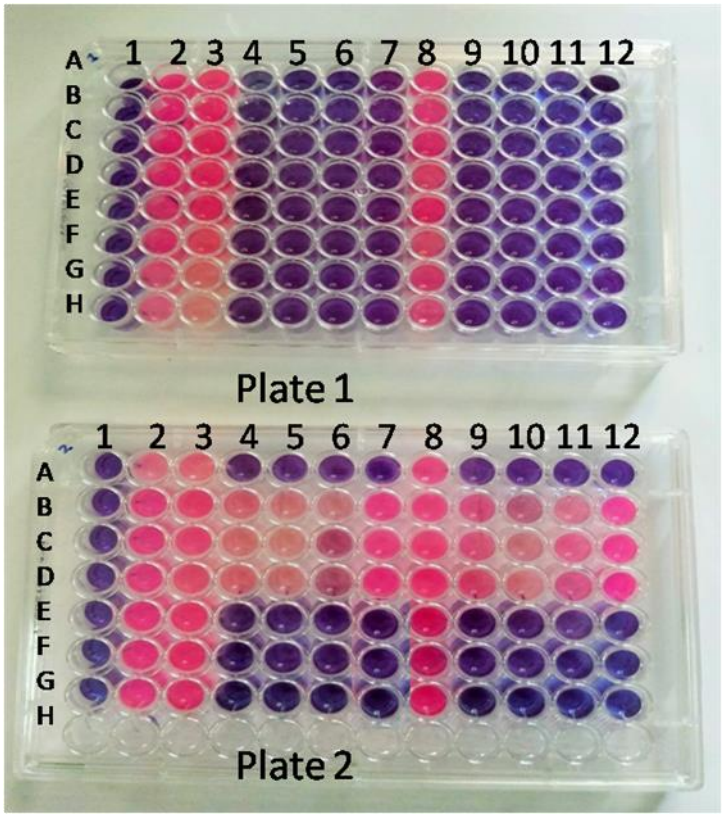

Figure 11. MIC by resazurin dye- Column 1: NB +resazurin, column 2: NB +resazurin+ pathogen, column 3: NB + *B. clausii* supernatant+ pathogen+ resazurin, column 4-7: NB+ pathogen + *B. clausii*AgNP (10µl, 20µl, 40µl 80µl)+resazurin, column 8: NB + B subtilis supernatant+ pathogen+ resazurin, column 9-12: NB+ pathogen + *B. subtilis*AgNP (10µl, 20µl, 40µl 80µl)+resazurin. Plate 1-Row A, B&C: *E. coli*, D, E& F: *S. typhi*, G, H and A (plate 2): *P.aeruginosa*, B, C & D: *S. aureus*, E, F & G: *K. pneumoniae.*

Confirmation of AgNp formation was done by analyzing its plasmon resonance. Usually, spherical silver nanoparticles show SPR peak between 420 and 450nm and the width of the band will be based on its size [1]. The SPR peaks of AgNPs were at 420 and 419 nm which primarily gives an idea that the nanoparticles are spherical in shape. Presence of metallic silver was confirmed by SEM EDX and the crystalline nature was confirmed by XRD. The shape and size of the nanoparticles were confirmed by TEM. Further FTIR spectrum was taken to identify the functional groups or organic molecules associated with the AgNPs. The bands correspond at 675 nm in *B. clausii* spectrum is of C-H bend which is absent in *B. subtilis* while all other peaks are common to both nanoparticles. Peaks between 1600-1683 corresponds to the stretching of C=C and between 2850- 3000 corresponds to C-H stretch. The protenaceous nature of the capping compound is revealed by N-H stretch of primary and secondary amines and amides in between 3100-3500nm.

The toxicity of AgNPs to humans is a great concern while using in medical appliances. Chemically synthesized pure silver nanoparticles are toxic to humans as effective as prokaryotes in at the same concentrations generally due to the generation of oxidative stress. Hamouda et al., [18] reported the production of biocompatible AgNPs from cyanobacteria effective in human colon cancer and breast cancer cell lines but nontoxic to normal cells. Such biocompatible AgNPs have immense biomedical applications. Bacterial AgNPs is a potent candidate against multidrug drug resistant clinical isolates [19]. Silver nanoparticles exerted more antibacterial activity than bulk silver due to its small size and high surface area. Interaction of AgNPs with bacteria causes physicochemical changes in the cell wall and thereby cell leakage. Smaller nanoparticles can penetrate into the cell and causes interaction with different components resulting in respiratory burst as well as protein dysfunctioning. The severity increases as the amount of Ag^+ ions released also increased [20]. Antibacterial activity is also concentration dependent as indicated in our results. The zone of inhibition is higher for 80µl (highest concentration used here) of nanoparticles than the lower concentrations. But *S. aureus* was resistant to all concentrations. This might be due to the thick layer of peptidoglycan on the cell wall. A comparative study by Chatterjee et al., [21] in *S. aureus* and *E. coli* treated with AgNPs showed that IC_{50} value of AgNP was higher for *S. aureus* and the death rate and delay in reproduction was less compared with *E. coli.* Even though the nanoparticles cannot kill *S. aureus*, it can inhibit the biofilm formation. Like all pathogen biofilms were inhibited, *S. aureus* biofilm formation was also inhibited by both nanoparticles. The antibiofilm property enhances its value for use in various catheters and dental materials thereby preventing the development of pathogen biofilms. It also acts as nanoacarriers for drug delivery in cancer and wound healing [22].

Like antibacterial activity, antioxidant properties of silver nanoperticles are also well studied. But the correlation between concentration of nanoparticles and antioxidant activity is not well understood. The DPPH scavenging activity of AgNPs decreased as the concentration increased. Similar results were obtained by Guntur et al., [23] where the lowest concentration of AgNP exhibited maximum scavenging activity. But the other study also suggested that the scavenging activity is not related to the concentration [24]. Mittal et al., [25] showed that antioxidant activity of plant mediated silver AgNP increased with concentration. However silver nanoparticles exhibits antioxidant activity by mimicking the enzymes like catalase and peroxidase [26].

Table 1. Zone of inhibition of pathogens by AgNPs.

Pathogens	Zone of inhibition in cm							
	Volume of *Bacillus clausii* AgNPs				Volume of *Bacillus subtilis* AgNPs			
	10µl	20µl	40µl	80µl	10µl	20µl	40µl	80 µl
E. coli	1.17 ± 0.05	1.26 ± 0.05	1.63 ± 0.05	2.06 ± 0.05	1.43 ± 0.05	1.56 ± 0.05	1.64 ± 0.05	1.83 ± 0.05
S. typhi	1.73 ± 0.05	1.84 ± 0.05	1.97 ± 0.05	2.64 ± 0.05	1.83 ± 0.05	1.93 ± 0.05	1.93 ± 0.05	2.13 ± 0.05
P. aeruginosa	1.34 ± 0.05	1.54 ± 0.05	1.73 ± 0.05	2.14 ± 0.05	1.05 ± 0.05	1.37 ± 0.05	1.74 ± 0.05	2.04 ± 0.05
S. aureus	0	0	0	0	0	0	0	0
K. pneumoniae	1.14 ± 0.05	1.53 ± 0.05	1.83 ± 0.05	2.07 ± 0.05	1.16 ± 0.05	1.44 ± 0.05	1.63 ± 0.05	1.84 ± 0.05

Table 2. Percentage inhibition of pathogen biofilm by *B. clausii* AgNPs.

Pathogens	Percentage Inhibition (%)				
	***B. clausii* supernatant xuosupernatant**	***B. clausii* AgNPs (in µl)**			
		80µL	40µL	20µL	10µL
E. coli	16.02 ± 1.07	78.39 ± 1.7	77.72 ± 0.67	75.5 ± 1.17	69.26 ± 1.6
S. typhi	12.44 ± 1.08	87.59 ± 0.99	85.65 ± 1.52	85.29 ± 0.91	84.33 ± 0.50
P. aeruginosa	1.19 ± 0.91	93.62 ± 0.47	93.52 ± 0.11	93.4 ± 0.25	92.86 ± 0.54
S. aureus	4.84 ± 0.68	85 ± 1.76	81.17 ± 1.55	76.91 ± 1.77	60.12 ± 1.10
K. pneumoniae	4.72 ± 1.02	97.19 ± 1.54	88.60 ± 0.71	83.77 ± 1.40	69.65 ± 0.98

Table 3. Percentage inhibition of pathogen biofilm by *B. subtilis*AgNPs.

Pathogens	Percentage Inhibition (%)				
	***B subtilis* supernatant**	***B. subtilis* AgNPs (in µl)**			
		80µL	40µL	20µL	10µL
E. coli	17.46 ± 1.57	53.92 ± 1.94	50.06 ± 1.55	40.11 ± 0.58	39.54 ± 0.99
S. typhi	12.08 ± 1.3	74.38 ± 0.95	73.67 ± 0.72	69.36 ± 0.72	67.06 ± 0.06
P. aeruginosa	6.88 ± 1.49	95.04 ± 0.89	94.57 ± 0.46	86.27 ± 0.31	84 ± 1.18
S. aureus	13.04 ± 1.59	81.71 ± 1.09	69.31 ± 0.35	28.29 ± 0.42	31.77 ± 1.37
K. pneumoniae	16.46 ± 1.23	93.39 ± 1.13	88.33 ± 1.77	78.63 ± 1.01	66.66 ± 0.79

Table 4. Percentage of DPPH scavenging shown by different volumes of nanoparticle samples.

AgNPs	Percentage of DPPH scavenging			
	80µl	40µl	20µl	10µl
***B. clausii*AgNPs**	19.31 ± 1.01	21.16 ± 0.90	29.18 ± 1.1	37.95 ± 1.56
***B. subtilis*AgNPs**	33.58 ± 1.08	42.29 ± 1.35	48.07 ± 1.8	49.02 ± 1.4

4. CONCLUSIONS

Silver nanoparticles are well known for their biomedical applications. Biosynthesis of AgNPs gives the benefit of reducing health risk and more biocompatibility. Biosynthesis gives an additional benefit of capping molecules which can improve the biological properties of AgNPs. The optimum size of 20- 50nm is the main characteristic that gives the antibacterial and antibioflm activity. Biofilm production is one of the major problems in medical appliances which can be minimized by coating biocompatible AgNPs on the surface. Antioxidant property gives an additional benefit by scavenging the free radicals in biological systems and thereby gives protection. Since the nanoparticles of *B. clausii* and *B. subtilis* are antibacterial in nature they can be used against multi drug resistant pathogens and thereby reducing the risk of spreading the strains.

5. REFERENCES

1. 1. Siddiqi, K.S.; Husen, A.; Rao, R.A.K. A review on biosynthesis of silver nanoparticles and their biocidal properties. *J Nanobiotechnology* **2018**, *16*, 14, https://doi.org/10.1186/s12951-018-0334-5.
2. Clement, J.L.; Jarrett, P.S. Antibacterial silver. *Met Based Drugs* **1994**, *1*, 467-482, https://doi.org/10.1155/mbd.1994.467.
3. Sim, W.; Barnard, R.T.; Blaskovich, M.A.T.; Ziora, Z.M. Antimicrobial Silver in Medicinal and Consumer Applications: A Patent Review of the Past Decade (2007(-)2017). *Antibiotics (Basel)* **2018**, *7*, https://doi.org/10.3390/antibiotics7040093.
4. Javaid, A.; Oloketuyi, S.F.; Khan, M.M.; Khan, F. Diversity of Bacterial Synthesis of Silver Nanoparticles. *BioNanoScience* **2018**, *8*, 43-59, https://doi.org/10.1007/s12668-017-0496-x.
5. FAO/WHO. Investigating the efficacy of network visualizations for intelligence tasks. In: *Probiotics in Food . Health and Nutritional Properties and Guidelines for Evaluation*. 2001..
6. Kalimuthu, K.; Suresh Babu, R.; Venkataraman, D.; Bilal, M.; Gurunathan, S. Biosynthesis of silver nanocrystals by Bacillus licheniformis. *Colloids and Surfaces B: Biointerfaces* **2008**, *65*, 150-153, https://doi.org/10.1016/j.colsurfb.2008.02.018.
7. Nithya, R. Synthesis of silver nanoparticles using a probiotic microbe and its antibacterial effect against multidrug resistant bacteria. *African J Biotechnol*. **2012,** *11*, 11013-11021.
8. Loo, Y.Y.; Rukayadi, Y.; Nor-Khaizura, M.A.; Kuan, C.H.;

Chieng, B.W.; Nishibuchi, M.; Radu, S. In Vitro Antimicrobial Activity of Green Synthesized Silver Nanoparticles Against Selected Gram-negative Foodborne Pathogens. *Front Microbiol* **2018**, *9*, 1555, https://doi.org/10.3389/fmicb.2018.01555.
9. Kaur, S.; Sharma, P.; Kalia, N.; Singh, J.; Kaur, S. Anti-biofilm Properties of the Fecal Probiotic Lactobacilli Against Vibrio spp. *Front Cell Infect Microbiol* **2018**, *8*, 120, https://doi.org/10.3389/fcimb.2018.00120.
10. Kalishwaralal, K.; BarathManiKanth, S.; Pandian, S.R.K.; Deepak, V.; Gurunathan, S. Silver nanoparticles impede the biofilm formation by Pseudomonas aeruginosa and Staphylococcus epidermidis. *Colloids and Surfaces B: Biointerfaces* **2010**, *79*, 340-344, https://doi.org/10.1016/j.colsurfb.2010.04.014.
11. Kumar, A.; Srivastava, R.; Singh, P.; Bahadur, V. Antioxidant and antibacterial activity of silver nanoparticles synthesized by Cestrum nocturnum. *J Ayurveda Integr Med*. **2018,** *11*, 1-8, https://doi.org/10.1016/j.jaim.2017.11.003.
12. Han, J.W.; Gurunathan, S.; Jeong, J.K.; Choi, Y.J.; Kwon, D.N.; Park, J.K.; Kim, J.H. Oxidative stress mediated cytotoxicity of biologically synthesized silver nanoparticles in human lung epithelial adenocarcinoma cell line. *Nanoscale Res Lett* **2014**, *9*, 459, https://doi.org/10.1186/1556-276x-9-459.
13. Kumar, B.; Angulo, Y.; Smita, K.; Cumbal, L.; Debut, A. Capuli cherry-mediated green synthesis of silver nanoparticles under white solar and blue LED light. *Particuology* **2016**, *24*, 123-128, https://doi.org/10.1016/j.partic.2015.05.005.
14. Roy, A.; Bulut, O.; Some, S.; Mandal, A.K.; Yilmaz, M.D. Green synthesis of silver nanoparticles: biomolecule-nanoparticle organizations targeting antimicrobial activity. *RSC Advances* **2019**, *9*, 2673-2702, https://doi.org/10.1039/C8RA08982E.
15. Rafique, M.; Sadaf, I.; Rafique, M.S.; Tahir, M.B. A review on green synthesis of silver nanoparticles and their applications. *Artif Cells Nanomed Biotechnol* **2017**, *45*, 1272-1291, https://doi.org/10.1080/21691401.2016.1241792.
16. Fang, X.; Wang, Y.; Wang, Z.; Jiang, Z.; Dong, M. Microorganism Assisted Synthesized Nanoparticles for Catalytic Applications. *Energies* **2019**, *12*, 190, https://doi.org/10.3390/en12010190.
17. Mukherjee, K.; Gupta, R.; Kumar, G.; Kumari, S.; Biswas, S.; Padmanabhan, P. Synthesis of silver nanoparticles by Bacillus clausii and computational profiling of nitrate reductase enzyme involved in production. *Journal of Genetic Engineering and Biotechnology* **2018**, *16*, 527-536, https://doi.org/10.1016/j.jgeb.2018.04.004.
18. Hamouda, R.A.; Hussein, M.H.; Abo-elmagd, R.A.; Bawazir, S.S. Synthesis and biological characterization of silver nanoparticles derived from the cyanobacterium Oscillatoria limnetica. *Scientific Reports* **2019**, *9*, 13071, https://doi.org/10.1038/s41598-019-49444-y.
19. Barros, C.H.N.; Fulaz, S.; Stanisic, D.; Tasic, L. Biogenic Nanosilver against Multidrug-Resistant Bacteria (MDRB). *Antibiotics (Basel)* **2018**, *7*, https://doi.org/10.3390/antibiotics7030069.
20. Qing, Y.; Cheng, L.; Li, R.; Liu, G.; Zhang, Y.; Tang, X.; Wang, J.; Liu, H.; Qin, Y. Potential antibacterial mechanism of silver nanoparticles and the optimization of orthopedic implants by advanced modification technologies. *Int J Nanomedicine* **2018**, *13*, 3311-3327, https://doi.org/10.2147/ijn.S165125.
21. Chatterjee, T.; Chatterjee, B.K.; Majumdar, D.; Chakrabarti, P. Antibacterial effect of silver nanoparticles and the modeling of bacterial growth kinetics using a modified Gompertz model. *Biochimica et Biophysica Acta (BBA) - General Subjects* **2015**, *1850*, 299-306, https://doi.org/10.1016/j.bbagen.2014.10.022.
22. Burdusel, A.C.; Gherasim, O.; Grumezescu, A.M.; Mogoanta, L.; Ficai, A.; Andronescu, E. Biomedical Applications of Silver Nanoparticles: An Up-to-Date Overview. *Nanomaterials (Basel)* **2018**, *8*, https://doi.org/10.3390/nano8090681.
23. Guntur, S.R.; Kumar, N.S.; Hegde, M.M.; Dirisala, V.R. In Vitro Studies of the Antimicrobial and Free-Radical Scavenging Potentials of Silver Nanoparticles Biosynthesized From the Extract of Desmostachya bipinnata. *Anal Chem Insights* **2018**, *13*, https://doi.org/10.1177/1177390118782877.
24. Otunola, G.A.; Afolayan, A.J. In vitro antibacterial, antioxidant and toxicity profile of silver nanoparticles green-synthesized and characterized from aqueous extract of a spice blend formulation. *Biotechnology & Biotechnological Equipment* **2018**, *32*, 724-733, https://doi.org/10.1080/13102818.2018.1448301.
25. Mittal, A.K.; Bhaumik, J.; Kumar, S.; Banerjee, U.C. Biosynthesis of silver nanoparticles: Elucidation of prospective mechanism and therapeutic potential. *Journal of Colloid and Interface Science* **2014**, *415*, 39-47, https://doi.org/10.1016/j.jcis.2013.10.018.
26. Li, J.; Liu, W.; Wu, X.; Gao, X. Mechanism of pH-switchable peroxidase and catalase-like activities of gold, silver, platinum and palladium. *Biomaterials* **2015**, *48*, 37-44, https://doi.org/10.1016/j.biomaterials.2015.01.012.

6. ACKNOWLEDGEMENTS

The authors are grateful to acknowledge DST PURSE Phase II programme Govt. of India, (No.SR/PURSE/Phase 2/26 (C)), DST FIST (No. SR/FST/LSI- 660/2016 (C)) and Kerala State Council for Science Technology and Environment (No.001/FSHP-MAIN/2015/KSCSTE) for providing funding and infrastructure facilities.